RESEARCH ARTICLE

Discovery of Norbornene as a Novel Hydrophobic Tag Applied in Protein Degradation

Shaowen Xie,[a] Feiyan Zhan,[a] Jingjie Zhu,[a] Yuan Sun,[a] Huajian Zhu,[a] Jie Liu,[e] Jian Chen,[b] Zheying Zhu,[d] Dong-Hua Yang,[c] Zhe-Sheng Chen,[c] Hong Yao,*[a] Jinyi Xu,*[a] and Shengtao Xu*[a, b]

[a] S. Xie, F. Zhan, J. Zhu, Y. Sun, H. Zhu, Prof. Dr. H. Yao, Prof. Dr. J. Xu, Prof. Dr. S. Xu
Department of Medicinal Chemistry,
School of Pharmacy, China Pharmaceutical University,
639 Longmian Avenue, Nanjing, Jiangsu 211198, China
E-mail: hyao1989@sina.cn (Prof. Dr. H. Yao), jinyixu@china.com (Prof. Dr. J. Xu), cpuxst@163.com (Prof. Dr. S. Xu)

[b] Prof. Dr. Chen, Prof. Dr. S. Xu
Department of Hepatobiliary Surgery,
The First People's Hospital of Kunshan,
Suzhou, Jiangsu 215132, China

[c] Prof. Dr. D. Yang, Prof. Dr. Z. Chen
College of Pharmacy and Health Sciences,
St. John's University,
Queens, New York 11439, United States

[d] Prof. Dr. Z. Zhu
Division of Molecular Therapeutics and Formulation,
School of Pharmacy, The University of Nottingham,
University Park, NG7 2RD, United Kingdom

[e] Prof. Dr. J. Liu
Department of Organic Chemistry,
School of Pharmacy, China Pharmaceutical University,
639 Longmian Avenue, Nanjing, Jiangsu 211198, China

Supporting information for this article is given via a link at the end of the document.

Abstract: Hydrophobic tagging (HyT) is a potential therapeutic strategy for targeted protein degradation (TPD). Norbornene was discovered as an unprecedented hydrophobic tag in this study and was used to degrade the anaplastic lymphoma kinase (ALK) fusion protein by linking it to ALK inhibitors. The most promising degrader, **Hyt-9**, potently reduced ALK levels through Hsp70 and the ubiquitin–proteasome system (UPS) *in vitro* without compensatory upregulation of *ALK*. Furthermore, **Hyt-9** exhibited a significant tumor-inhibiting effect *in vivo* with moderate oral bioavailability. More importantly, norbornene can also be used to degrade the intractable enhancer of zeste homolog 2 (EZH2) when tagged with the EZH2 inhibitor tazemetostat. Thus, the discovery of novel hydrophobic norbornene tags shows promise for the future development of TPD technology.

Introduction

Since the first report of proteolysis-targeting chimera (PROTAC) molecules in 2001, targeted protein degradation (TPD) has emerged as a therapeutic strategy to overcome intractable disease-causing proteins.[1] In particular, the published trial data of ARV-110 and ARV-471, androgen receptor (AR), and estrogen receptor (ER)-degrading PROTACs, started an era of rationally designed TPD molecules for potential human therapeutic applications.[2] However, the widespread application of PROTACs is limited owing to their poor cellular permeability, pharmacokinetics (PKs), and bioavailability, which is largely attributed to their high molecular weight (usually in the range of 700-1,000 Da).[3]

As a promising therapeutic strategy for designing TPD molecules that have long been underestimated, hydrophobic tagging (HyT) technology offers several advantages over PROTACs,[4] including lower molecular weight and elimination of the risk of teratogenic side effects from thalidomide-derived cereblon (CRBN) ligands.[5] A typical HyT molecule consists of two components: one is an identifying peptide or small-molecule chemical ligand that specifically binds to the protein of interest (POI), and the other is a hydrophobic tag that mimics a misfolded protein state thus leading to the degradation of POI by recruiting chaperones or proteasomes.[6]

A small number of hydrophobic tags such as adamantane,[7] fluorene,[8] pyrene,[9] tert-butyl carbamate-protected arginine (Boc_3Arg),[10] carborane,[11] and menthoxyacetyl[12] have been discovered and successfully employed in the design of HyT degraders targeting several POIs, including AR,[7a] human epidermal growth factor receptor 3 (HER3, also known as ErbB3),[7b, 7c] enhancer of zeste homolog 2 (EZH2),[7d] HaloTag,[7e, 13] poly (ADP-ribose) polymerase 1 (PARP1),[8] Tau,[14] retinal rod rhodopsin-sensitive cGMP 3',5'-cyclic phosphodiesterase subunit delta (PDEδ),[15] steroid receptor coactivator-1 (SRC-1),[16] protein kinase B (Akt),[17] and polo-like kinase 1 (PLK1)[18]. However, most of the hydrophobic moieties mentioned above exhibit poor physicochemical or PK properties.[6a] Additionally, low bioavailability leads to incomplete degradation of the POI, which may represent a major challenge for the extensive application and clinical development of HyT molecules.[19] In addition, the limited

number of usable HyT tags restricts the scope of available targets for HyT technology. The discovery of novel hydrophobic tags with superior druggability and degradation efficiency is important for improving TPD therapeutic outcomes.

Results and Discussion

Our laboratory reported an alectinib (**A1**)-based PROTAC, **Q2** (Supporting Information, Figure S1A), which was designed using CRBN ligands to degrade anaplastic lymphoma kinase (ALK).[20] ALK is a desirable target for cancer therapy because of its significant involvement in a variety of malignancies, as well as its low expression in adult tissues.[21] **Q2** potently mediates ALK fusion protein degradation in cells and effectively reduces ALK fusion protein levels in tumor tissues. However, further development of **Q2** stagnated, as the large size of **Q2** led to poor drug-likeness. Herein, we attempted to apply HyT technology to improve the poor physicochemical and PK properties of **A1**-based TPD molecules. By using time-resolved fluorescence resonance energy transfer (TR-FRET) and [3-(4,5-dimethylthiazol-2-yl)-2,5-diphenyltetrazolium bromide] (MTT) methods, we found an **A1** derivative **A3**, which bears a piperazine group and exhibits higher affinity for ALK and more potent antiproliferative activity *in vitro* than **A1** (ALK binding affinities (IC_{50}): **A1** = 1.03 ± 0.29 nM, **A3** = 0.32 ± 0.04 nM; H3122 cells (IC_{50}): **A1** = 47 ± 1 nM, **A3** = 46 ± 2 nM, Supporting Information, Figure S1B), we chose **A3** as a POI ligand to append the potential hydrophobic moieties to explore our assumption (Supporting Information, Figure S1C). Thus, a series of novel hydrophobic-tagged ALK degraders was further synthesized by connecting various potential hydrophobic tags, such as adamantane,[7a-d] indacen, fluorene,[8] Boc_3Arg,[10] oleic acid, and norbornene, to **A3** with alkyl acid as the linker (Table 1).

Table 1. ALK binding affinities, antiproliferative activities and ALK degradation abilities of ALK HyT degraders in H3122 cells.

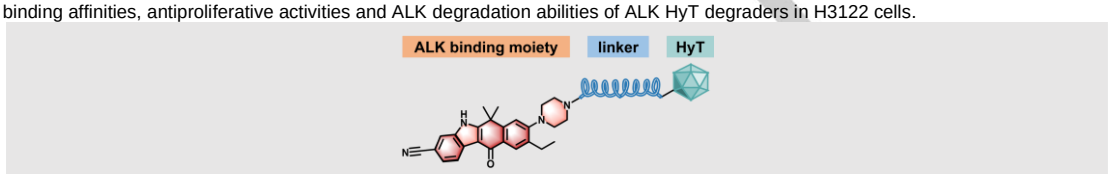

cpds	Linker + Hydrophobic tag	ALK binding affinities (nM)[a]	H3122 cell line			
			IC_{50} (μM)[b]	EML4-ALK degradation %[c]		
				0.5 μM	1 μM	5 μM
Hyt-1	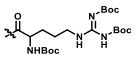	810.26 ± 12.45	> 10	-2.2 ± 1.5	5.4 ± 1.5	5.7 ± 4.8
Hyt-2	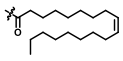	672.10 ± 45.90	> 10	-2.0 ± 2.8	-3.8 ± 1.9	-7.1 ± 5.3
Hyt-3		116.97 ± 4.21	1.33 ± 0.29	40.9 ± 10.8	45.8 ± 5.9	59.2 ± 1.4
Hyt-4		302.80 ± 20.65	6.01 ± 0.79	62.2 ± 4.4	63.1 ± 6.4	65.5 ± 15.4
Hyt-5		122.03 ± 2.33	1.44 ± 0.21	45.2 ± 15.7	59.6 ± 28.1	68.8 ± 14.9
Hyt-6	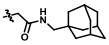	66.42 ± 0.01	0.75 ± 0.28	49.5 ± 19.2	76.1 ± 2.9	84.0 ± 1.0
Hyt-7		38.88 ± 2.03	0.14 ± 0.01	70.4 ± 3.8	74.5 ± 2.1	77.1 ± 1.7
Hyt-7i		55.55 ± 5.11	0.90 ± 0.01	41.6 ± 10.0	54.8 ± 10.7	58.8 ± 3.6

[a]ALK binding affinities of the compounds were measured using TR-FRET ALK kinase assays. IC_{50} values are shown when calculated using the variable slope equation in GraphPad Prism 8. [b]IC_{50} values (means ± SD) were obtained from three independent experiments using the MTT method with a treatment time of 72 h in H3122 cells. [c] EML4-ALK degradation % = 100 − EML4-ALK relative protein levels (%). EML4-ALK relative protein levels were detected by western blotting, quantified by densitometric analysis using ImageJ, and normalized against GAPDH levels from three independent experiments performed in H3122 cells after treatment with various concentrations (0.5, 1, and 5 μM) of compounds for 24 h.

A3-based HyT molecules were successfully synthesized using the process shown in Scheme S1 (Supporting Information). We then assessed the antiproliferative activities and protein degradative potency (Table 1, Supporting Information, Figure S2) of these degraders in EML4 (echinoderm microtubule-associated protein-like 4)-ALK fusion-positive H3122 cells. **Hyt-1** and **Hyt-2** did not mediate EML4-ALK degradation after incubation with H3122 cells at a concentration of 5 μM or less for 24 h. Accordingly, these two HyT molecules did not show obvious potency in inhibiting the growth of H3122 cells (IC_{50} > 10 μM). Interestingly, compounds **Hyt-3** and **Hyt-4** with aromatic moieties as hydrophobic tags, exhibited moderate degradative potency and reduced EML4-ALK expression by approximately 60% at a concentration of 5 μM. Correspondingly, the antiproliferative activities in H3122 cells were also improved (**Hyt-3**: IC_{50} = 1.33 ± 0.29 μM, **Hyt-4**: IC_{50} = 6.01 ± 0.79 μM, Table 1). Compounds **Hyt-5** and **Hyt-6** were designed and synthesized by linking an adamantane moiety, which is the most widely reported

hydrophobic tag, to the ALK ligand **A3** with different linker lengths. Indeed, compound **Hyt-5** effectively induced EML4-ALK degradation by > 65% at 5 μM and maintained favorable antiproliferative activity in H3122 cells (IC_{50} = 1.44 ± 0.21 μM). Moreover, compound **Hyt-6**, which has only one more methylene group than **Hyt-5**, showed an approximately 2-fold increase in ALK binding affinity and antiproliferative activity compared to **Hyt-5** (Table 1, Supporting Information, Figure S3).

Compound **Hyt-7**, tagged with norbornene, which has the lowest molecular weight to date (Supporting Information, Figure S4), showed the most potent degradative potency at a concentration of 0.5 μM compared with other HyT degraders, with > 70% degradation of EML4-ALK in H3122 cells. Moreover, **Hyt-7** exhibited the most potent ALK-binding affinity and antiproliferative activity in H3122 cells among the HyT degraders. In addition, except for EML4-ALK, **Hyt-7** potently degraded the nucleophosmin (NPM)-ALK fusion protein in SU-DHL-1 cells at a concentration of 0.5 μM after 48 h of treatment (Supporting Information, Figure S5). To further explore whether the double bond in norbornene contributes to the degradative potency of **Hyt-7**, we designed and synthesized a hydrogenated norbornene-based HyT degrader, **Hyt-7i** (Table 1, Supporting Information, Scheme S1). The degradative effects of **Hyt-7i** at the given concentrations were less than those of **Hyt-7** (Supporting Information, Figure S6). Accordingly, the antiproliferative activity of **Hyt-7i** was also decreased (Table 1). These results indicated that the double bond in norbornene plays a critical role in its degradative potency.

The differences in the degradative and antiproliferative activities of **Hyt-5** and **Hyt-6** indicated that the contribution to the potency in ALK degradation and anti-proliferative effects made by the length of the linker could not be neglected. Therefore, we investigated an optimal linker for fusion with norbornene. Compounds **Hyt-8~10** which incorporated linkers of different lengths, were synthesized (Figure 1A, Supporting Information, Scheme S2). Western blotting assays showed that compounds **Hyt-7~10** maintained good potency in degrading EML4-ALK by >60% at a concentration of 0.5 μM in H3122 cells. Specifically, compound **Hyt-9** degraded 74% of EML4-ALK at a concentration of 0.5 μM in H3122 cells (Figure 1B). Moreover, compound **Hyt-9** exhibited more potent antiproliferative activity in H3122 cells, with an IC_{50} value of 0.07 ± 0.01 μM (Figure 1C). Therefore, according to western blotting and antiproliferative data, we selected the most potent compound, **Hyt-9**, as the representative compound for further *in vitro* and *in vivo* studies and mechanistic investigations.

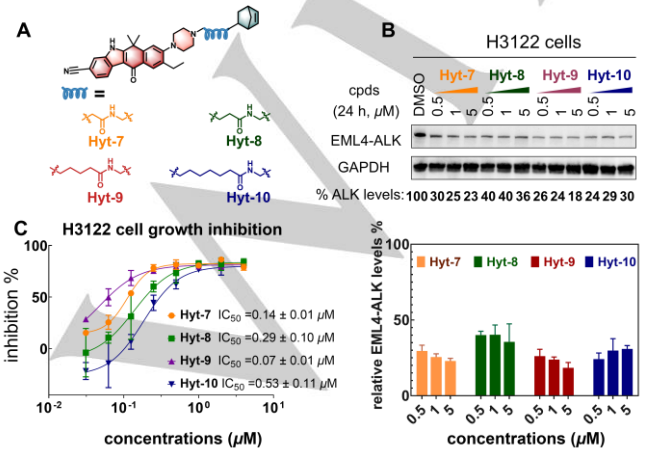

Figure 1. Design and biological evaluation of compounds **Hyt-7~10**. (A) Structures of norbornene-based degraders **Hyt-7~10**. (B) Effects of degraders **Hyt-7~10** on reducing EML4-ALK protein levels in H3122 cells at the indicated concentrations for 24 h (upper panel). Mean values and SDs from three independent experiments are shown (lower panel). EML4-ALK levels were normalized to EML4-ALK levels in dimethyl sulfoxide (DMSO). (C) Cell growth inhibition in H3122 cells. Cells were treated with the indicated concentrations of compounds **Hyt-7~10** for 72 h (0.032, 0.063, 0.125, 0.250, 0.500, 1.000, 2.000, and 4.000 μM from left to right), and IC_{50} values were determined using MTT assays. Data are presented as means ± SD of three independent experiments.

Interestingly, compound **Hyt-9** potently induced EML4-ALK protein degradation in a dose-dependent manner with a DC_{50} of 134 nM after 24 h of treatment (Figure 2A, B), whereas other reported degraders based on known HyTs could only degrade the POI at submicromolar or micromolar levels (Supporting Information, Table S1).[7a, 8, 10a, 18] In addition, **Hyt-9** could comprehensively inhibit ALK phosphorylation at a low concentration of 50 nM in H3122 cells, which is comparable to **A1**-based PROTACs at the same concentration that have been reported.[20] Time-response curves indicated that **Hyt-9** potently inhibited ALK phosphorylation (100% inhibition) after approximately 2 h of treatment. A maximum degradation of approximately 95% of EML4-ALK protein was observed after incubation with 1 μM **Hyt-9** for 48 h (Figure 2C, D). Washout experiments were performed to assess sustained cellular degradative activity produced by **Hyt-9**. In H3122 cells, EML4-ALK protein levels were reduced to 24% after 24 h of treatment with 1 μM **Hyt-9**, and EML4-ALK protein was maintained at a low level without any recovery after removal of the degraders for 48 h (Figure 2E, F). These findings revealed that the degrader **Hyt-9** has a long-lasting or post-dosing effect on the degradation of EML4-ALK, highlighting implications in clinical dosing regimens by reducing dose frequency, leading to reduced side effects of ALK inhibitors and delivering superior efficacy at lower cost.

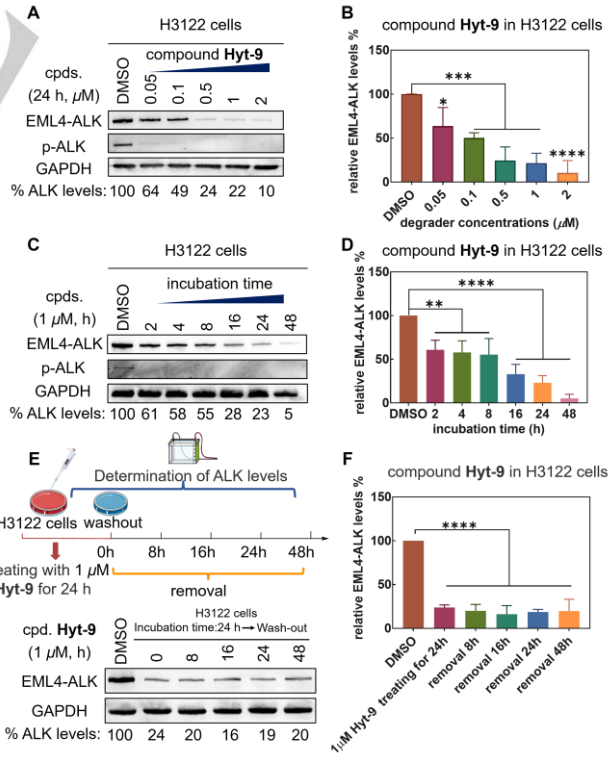

Figure 2. Evaluation of **Hyt-9** degradation in H3122 cells. **(**A) Compound **Hyt-9** reduced EML4-ALK levels and inhibited ALK phosphorylation in a concentration-dependent manner. (C) Compound **Hyt-9** reduced EML4-ALK levels in a time-dependent manner and inhibits ALK phosphorylation. (E) Schematic illustration of the schedule for drug removal in H3122 cells.

Sustained cellular degradative activity induced by compound **Hyt-9** upon washout in H3122 cells. Cells were treated with compound **Hyt-9** at the indicated times and concentrations, washed with phosphate-buffered saline (PBS) three times, and harvested at the indicated time points for western blot analysis. (B), (D), (F) Quantitation of the data shown in (A), (B), (C). Mean values and SDs from three independent experiments are shown. EML4-ALK levels were normalized relative to EML4-ALK levels in DMSO. Significance is shown as $*p < 0.05$, $**p < 0.01$, $***p < 0.001$, and $****p < 0.0001$ compared to the vehicle-only treated group.

To further verify the capacity of compound **Hyt-9** in ALK degradation and inhibition of ALK phosphorylation in H3122 cells, we conducted immunofluorescence experiments. Consistent with earlier immunoblotting results, the fluorescence intensity of ALK and p-ALK was significantly reduced after treating H3122 cells with 0.5 μM compound **Hyt-9** for 24 h, which was normally visible in DMSO-treated cells (Figure 3A, B). Next, real-time quantitative polymerase chain reaction (RT-qPCR) was performed to identify whether the downregulation of EML4-ALK mediated by **Hyt-9** was at the protein or gene expression level. As shown in Figure 3C, the mRNA level of *ALK* in H3122 cells after treatment with 0.5 μM of the **A1**-based PROTAC **Q2** or the **A1**-based HyT degrader **Hyt-9** at the indicated concentrations was not decreased compared with that of the vehicle control. After treatment with 0.5 μM of the ALK inhibitor **A1**, the mRNA levels of *ALK* showed an approximately 2-fold increase compared to those of the vehicle control or other degrader groups. These results indicated that the downregulation of EML4-ALK was mediated at the protein level via degraders **Q2** or **Hyt-9**. The rate of protein degradation induced by **Hyt-9** was more rapid than the *de novo* synthesis of proteins mediated by transcription. This compensatory upregulation of *ALK* may be caused by antagonization by ALK inhibitors.[3a] Even a short inhibition time via an inhibitor of its POI can lead to target accumulation, resulting in drug resistance, which is detrimental to the efficacy of ALK inhibitors.[22] More importantly, the elimination of POI with HyT is expected to be particularly suitable for proteins that are compensatorily upregulated via inhibitors, which could open a new avenue for overcoming drug resistance mediated by protein stabilization or overexpression. Flow cytometric analysis was conducted to investigate the effects of the degrader **Hyt-9** on the cell cycle of H3122 cells (Figure 3D, E). The percentage of G1 cells after treatment with 0.1 μM or 0.5 μM of the degrader **Hyt-9** for 24 h was significantly lower than the percentage of G1 cells after treatment with vehicle control. Notably, after treatment with 0.5 μM of the degrader **Hyt-9** for 24 h, H3122 cells showed a prominent sub-G0 population representing apoptotic cells. Inspired by this result, Annexin V-FITC/PI was used to further investigate the ability of the ALK degrader **Hyt-9** to induce apoptosis in H3122 cells (Figure 3F, G). The degrader **Hyt-9** exhibited a dose-dependent increase in apoptosis of H3122 cells after 24 h of incubation. In particular, robust apoptosis of H3122 cells was observed after treatment with 0.5 μM of the degrader **Hyt-9** for 24 h, consistent with its effect on cell cycle arrest. Thus, **Hyt-9** potently degraded EML4-ALK protein, inducing cell death via apoptosis.

WILEY-VCH

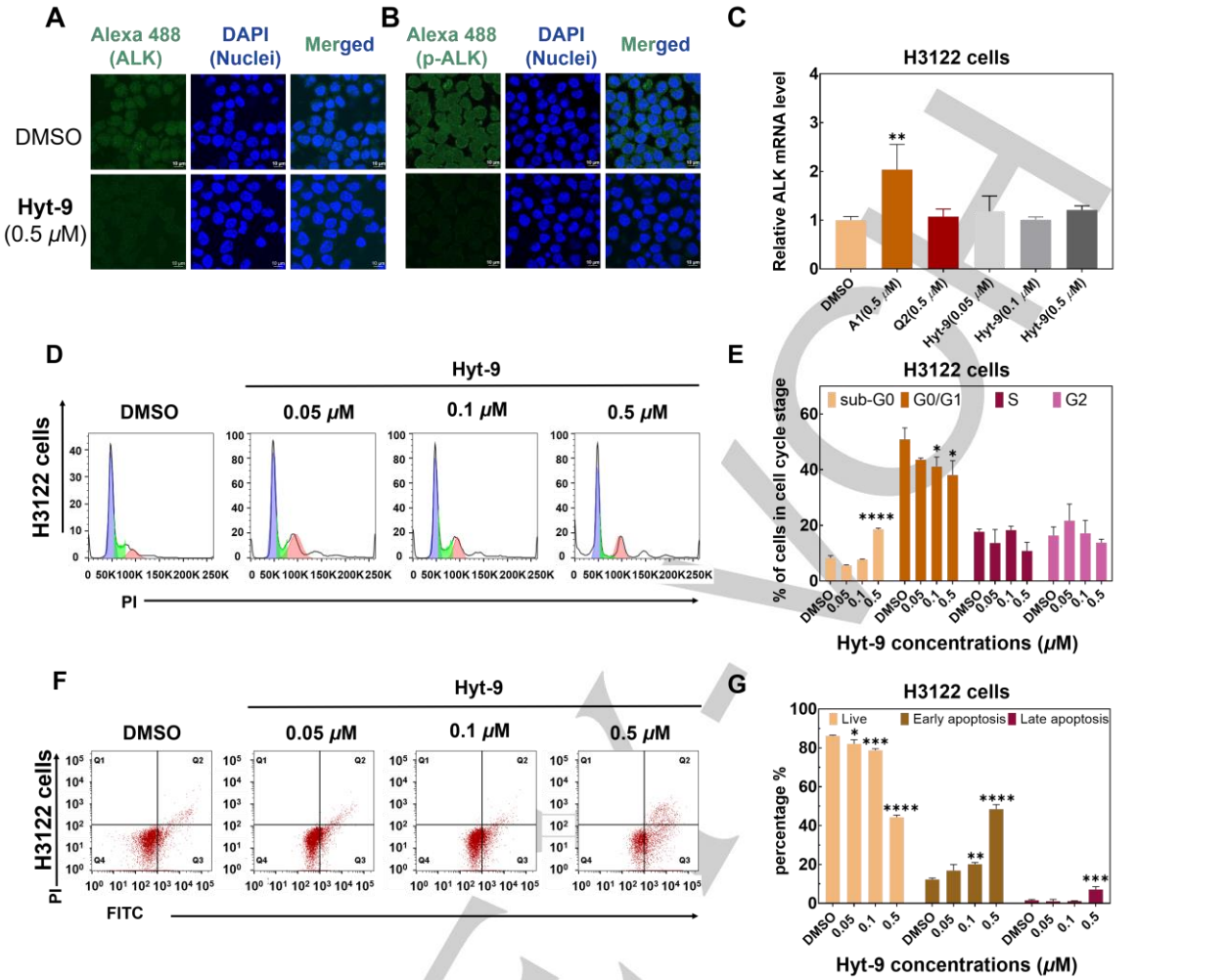

Figure 3. Immunofluorescence staining of (A) ALK and (B) p-ALK in untreated H3122 cells (DMSO, upper panel) or cells treated with 0.5 μM degrader **Hyt-9** (lower panel) for 24 h. Nuclei were counterstained with 4',6-diamidino-2-phenylindole (DAPI). ALK and p-ALK were counterstained with Alexa 488. Merged images are shown in the right column. In representative images, the scale bar is 10 μm. (C) H3122 cells were treated with DMSO, **A1** (0.5 μM), **Q2** (0.5 μM), or **Hyt-9** (0.05, 0.1, 0.5 μM) for 24 h and harvested for real-time qPCR. Data are presented as the mean ± SD (n = 3 independent experiments). (D) H3122 cells were treated with compound **Hyt-9** at concentrations of 0.05, 0.1, and 0.5 μM for 24 h. Then, the cells were fixed in ice-cold 70% ethanol at 4 °C and stained with propidium iodide (PI) dye, and the cell cycle was evaluated via flow cytometry. (E) The bar graph shows the percentages of cells in sub-G0, G0/G1, S, and G2 phases. (F) Flow cytometry of apoptotic cells induced by the indicated concentrations of the compound **Hyt-9** for 24 h and stained with Annexin V - fluorescein isothiocyanate (FITC)/PI in H3122 cells. (G) The bar graph shows the percentages of apoptotic cells. Significance is shown as *$p < 0.05$, **$p < 0.01$, ***$p < 0.001$, and ***$p < 0.0001$ compared to the vehicle-only treated group.

To investigate the mechanism of the degradation of **Hyt-9** in H3122 cells, we performed rescue assays. Pretreatment with the proteasome inhibitor MG-132 (2 μM) blocked ALK degradation induced by **Hyt-9** in H3122 cells (Figure 4A), suggesting that engagement of the proteasome pathway is essential for the observed ALK degradation. Pretreatment with the lysosomal inhibitor chloroquine did not affect ALK degradation (Figure 4A), suggesting that norbornene-induced degradation does not involve autophagy/lysosome pathways. Co-immunoprecipitation (Co-IP) pulldown experiments were performed to evaluate the possible involvement of Hsp70, given its known role in stabilizing or degrading misfolded proteins via the proteasome.[7a] [23] After treatment with **Hyt-9** for 24 h, we detected enhanced interactions between ALK and Hsp70 or ubiquitin (Figure 4B). To further explore the possibility of binding norbornene to Hsp70, we designed and synthesized a norbornene-biotin conjugate (**JBP-BIO**) and apoptozole-biotin conjugate (**AZ-BIO**) by connecting biotin to HyT norbornene and Hsp70 inhibitor apoptozole, respectively (Figure 4C, Supporting Information, Scheme S3 and S4).[24] **JBP-BIO** and **AZ-BIO** were incubated with proteins extracted from H3122 cells, followed by affinity enrichment using streptavidin magnetic beads, and validated by western blotting with an anti-Hsp70 antibody. As shown in Figure 4D, **JBP-BIO** did not directly bind to Hsp70 compared with the positive control **AZ-BIO**. Moreover, a thermal shift binding assay, which is based on stabilization and protection of the target protein from aggregation and/or precipitation at high temperatures upon binding to the small molecule, also showed that **Hyt-9** did not directly bind to Hsp70, as demonstrated by an insignificant increase in the thermal stability of the target protein compared with that of the DMSO group (Figure 4E).[25] These results suggested that ALK degradation caused by norbornene-based HyT was mediated by inducing the destabilization of ALK, thereby recruiting Hsp70 without directly binding and then degrading the protein by the proteasome (Figure 4F), and the precise mechanism of degradation warrants further investigation.

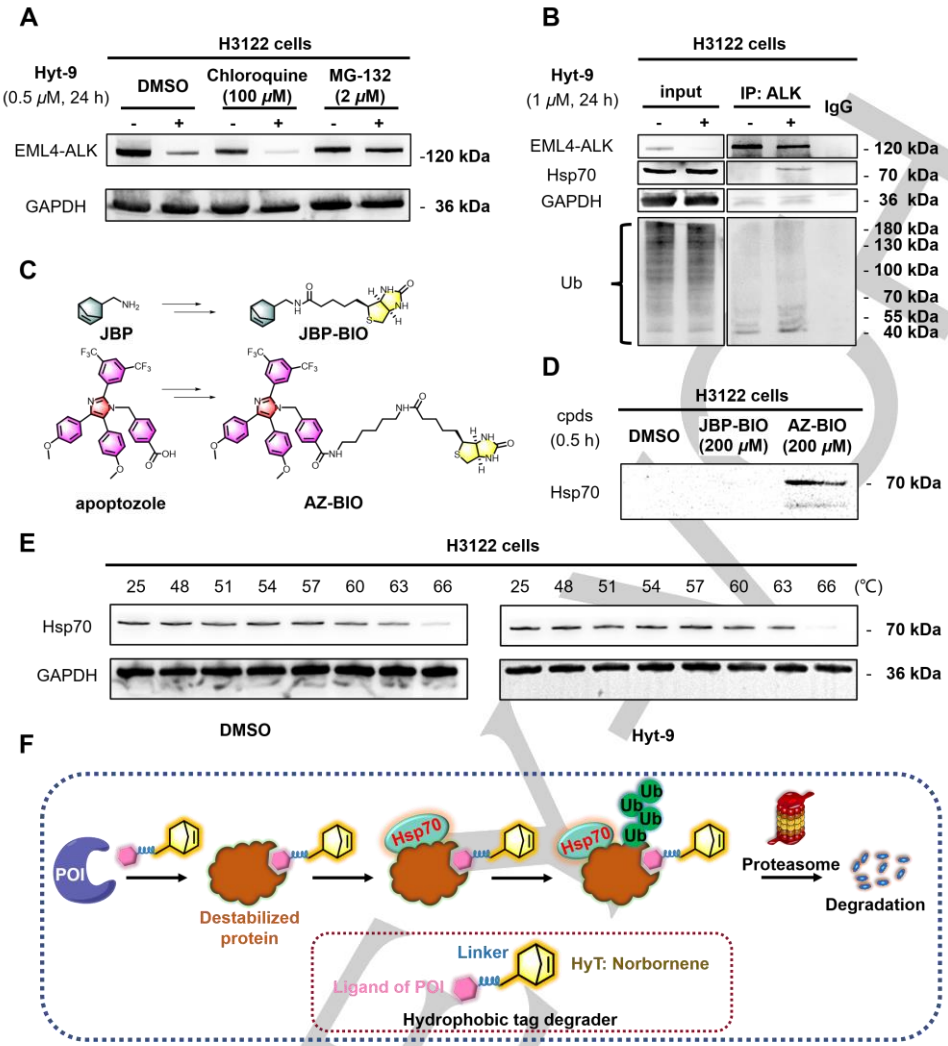

Figure 4. The degrader **Hyt-9** induces ALK degradation through Hsp70 and the UPS. (A) H3122 cells were pretreated with DMSO, chloroquine (100 μM), or MG-132 (2 μM) for 4 h before treatment with the degrader **Hyt-9** (0.5 μM) for an additional 24 h. Western blot results are representative of three independent experiments. (B) H3122 cells were pretreated with the degrader **Hyt-9** for 24 h. Cells were harvested for immunoprecipitation, and an ALK antibody was used to pull-down ALK with immunoglobulin G (IgG) as a negative control. Proteins were analyzed by western blotting using anti-ALK, anti-Hsp70, and anti-Ub antibodies. Western blotting results are representative of at least three independent experiments. (C) Structures of norbornene-biotin conjugate (**JBP-BIO**) and apoptozole-biotin conjugate (**AZ-BIO**). (D) Western blot results for target validation of norbornene in protein extracts from H3122 cells, and norbornene was not found to bind directly with Hsp70. (E) Thermal shift binding assay to evaluate the binding possibility of **Hyt-9** (200 μM) with Hsp70 in H3122 cells after incubation for 60 min. (F) Model for norbornene-mediated protein degradation.

Given the low molecular weight of norbornene, we assumed that norbornene-based HyT molecules might possess PK profiles superior to those of PROTACs. The stability of **Hyt-9** was investigated and was found to be extremely stable in mouse and human plasma (Supporting Information, Table S2). Moreover, the PK study of **Hyt-9** was conducted by single-dose intravenous (I.V.) and intragastric (P.O.) administration (Supporting Information, Table S3). PK data following a single I.V. administration of **Hyt-9** at 1 mg/kg achieved a maximum plasma concentration of 200.4 ng/mL. The clearance (CL) of 41.4 mL/min/kg and $t_{1/2}$ of 4.29 h were further improved compared with the results of **A1**-based PROTACs (I.V. (**Q2**): CL = 137.6 mL/min/kg; $t_{1/2}$ = 0.42 h), as previously reported by our group.[20] Importantly, we found that compound **Hyt-9** could be detected in plasma with acceptable oral bioavailability (F = 8.6%) and moderate $t_{1/2}$ (5.45 h) following P.O. administration (Supporting Information, Table S3). In brief, these results indicated that the molecular mass and number of hydrogen-bond donors/receptors of PROTACs could be reduced through the conversion of E3 ligase ligands into hydrophobic tags, thus reasonably improving the otherwise poor PK profiles of PROTACs.

Next, we evaluated the PD effect of **Hyt-9** *in vivo* in BALB/c nude mice bearing H3122 xenograft tumors. Ten mice bearing approximately 90 mm^3 H3122 xenograft tumors were randomly assigned to five groups (two animals in each group) and treated with a single dose of **Hyt-9** (10 mg/kg) via intravenous injection. The mice were sacrificed at 0, 12, 24, 36, and 48 h, and tumor samples were collected and probed for ALK expression levels (Supporting Information, Figure S7). Western blot data showed that a single administration of **Hyt-9** (I.V., 10 mg/kg) significantly decreased EML4-ALK fusion protein levels to 32.1 ± 11.5% at 36 h, and was effective in inducing near-complete elimination (7.2 ± 0.7% remaining) until 48 h (maximal observed time point).

Based on the results of drug removal experiments *in vitro* and PK/PD studies *in vivo* involving **Hyt-9**, we further explored its antitumor capability in an H3122 xenograft mouse model. Mice were treated once daily for 21 days at the indicated doses and

routes of administration (Figure 5). Both the positive control group and the **Hyt-9**-treated group showed significantly reduced tumor volumes and weight, with a tumor growth inhibition rate of approximately 50.7%-65.9% compared with the vehicle control group (Figure 5A, B, and C). In addition, none of the treatment groups exhibited significant body weight loss or other signs of toxicity (Figure 5D; Supporting Information, Figure S8). To determine the correlation between ALK degradation and tumor growth inhibition, we performed western blot analysis of xenograft tumor tissue to assess EML4-ALK degradation. Western blot data (Figure 5E, F) showed no significant difference in EML4-ALK fusion protein levels between the vehicle control group and the **A1**-treated group. However, all **Hyt-9**-treated groups effectively reduced the level of the EML4-ALK fusion protein in the xenograft tumor tissue with an unconsumed protein level of 38.4 ± 6.7% (**Hyt-9**: I.V., 5 mg/kg), 16.6 ± 7.3% (**Hyt-9**: I.V., 10 mg/kg), and 29.1 ± 12.3% (**Hyt-9**: P.O., 20 mg/kg).

Furthermore, we investigated whether **Hyt-9** could exhibit advantages over ALK inhibitor **A1**, **A1**-based PROTAC **Q2**, and adamantane-based HyT **Hyt-6** administered P.O. every other day for 21 days **(**Supporting Information, Figure S9**)**. **Hyt-9** (20 mg/kg) potently inhibited tumor growth with a tumor inhibition rate of 58.03%, which was superior to that of **A1** (42.20%), **Q2** (44.61%), and **Hyt-6** (43.12%) at the same dosing schedule (Supporting Information, Figure S9A, B, and C). In addition, no significant body weight loss was observed in any of the treated groups (Supporting Information, Figure S9D). Taken together, these two efficacy experiments suggested that **Hyt-9** could effectively penetrate and function in tumor tissue after P.O. administration and was more efficacious than the ALK inhibitor **A1**.

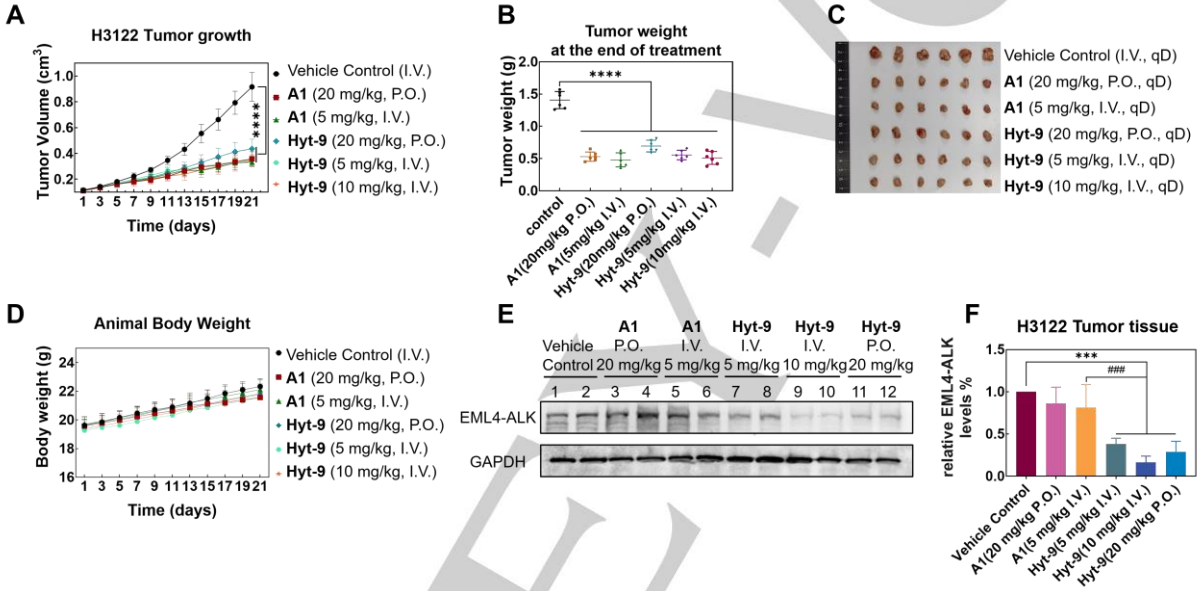

Figure 5. *In vivo* antitumor activity evaluation of **Hyt-9** in an H3122 xenograft mouse model. (A) Tumor growth ($^{****}p < 0.0001$ vs. vehicle control). (B) Weight of excised tumors from each group ($^{****}p < 0.0001$ vs. vehicle control). (C) Images of H3122 mouse tumors 21 days after initiation of treatment. (D) Body weight changes in mice during treatment. (E) Immunoblotting of H3122 xenograft tumor tissue after 21 days of treatment. (F) Quantification of EML4-ALK fusion protein levels in tumor tissue. The EML4-ALK levels were normalized relative to those of EML4-ALK in DMSO ($^{***}p < 0.001$ vs. vehicle control group, $^{###}p < 0.001$ vs. **A1** 5 mg/kg I.V. group).

Moreover, the degradative and inhibitory effects of compound **Hyt-9** on H3122 xenograft tumors after daily dosing for 21 days were further investigated by immunofluorescence staining of tumor tissues. As shown in Figure 6A, only the **Hyt-9**-treated groups had significantly reduced total ALK levels compared to the vehicle control and positive control groups. The decrease in ALK phosphorylation in **Hyt-9**-treated groups was greater than that in the vehicle-only treated control group (Figure 6B). The results of immunofluorescence staining were consistent with the earlier western blot results *in vitro* and *in vivo* (Figures 2 and 5E-F). Furthermore, the results from the terminal deoxynucleotidyl transferase dUTP nick end labeling (TUNEL) assay showed that **Hyt-9** induced significant apoptosis in tumor tissue cells via P.O. or I.V. administration compared to the vehicle control, which was comparable to the apoptosis levels in tumor tissue cells of the **A1**-treated groups (Figure 6C). Thus, **Hyt-9** could significantly inhibit tumor growth in an H3122 xenograft mouse model via I.V. or P.O. through induction of apoptosis.

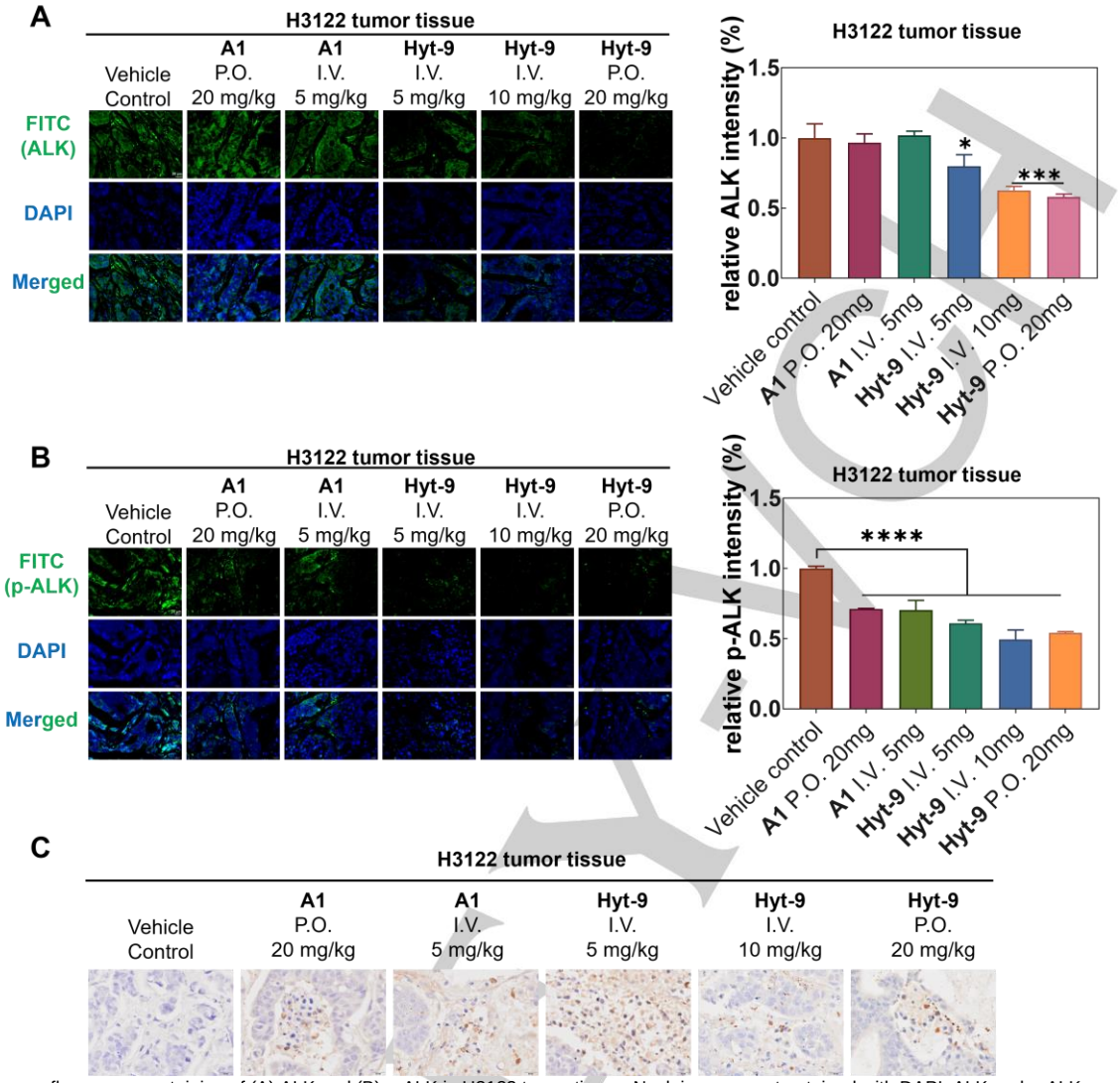

Figure 6. Immunofluorescence staining of (A) ALK and (B) p-ALK in H3122 tumor tissue. Nuclei were counterstained with DAPI. ALK and p-ALK were stained with FITC. The scale bar indicates 20 μm. Mean gray values were calculated using ImageJ from three independent experiments and compared to the related vehicle control group. Significance is shown as *$p < 0.05$, ***$p < 0.001$, and ****$p < 0.0001$ compared to the vehicle-only treated group. (C) Apoptosis in H3122 tumor tissue cells was assessed by TUNEL. Representative image of TUNEL staining of H3122 tumor tissue cells.

ALK is rarely expressed in healthy adult tissues but is overexpressed in some diseased tissues, making it a desirable target with high efficacy and minimal toxicity.[26] To assess the safety of the ALK degrader, we conducted an antiproliferative assay of **A1**, **Q2**, and **Hyt-9** in HFL-1 and A549 cells, which are ALK fusion-negative cells. The results demonstrated that **Hyt-9** had a minimal antiproliferative effect on ALK fusion-negative cells at concentrations of 1 and 10 μM compared to that of **A1** and **Q2** (Figure 7A, B). Although **A1** is a well-known ALK inhibitor with good kinase selectivity, it also inhibits leukocyte tyrosine kinase (LTK) and cyclin G-associated kinase (GAK), which have the highest sequence similarity to ALK.[27] To test the kinase selectivity of the ALK degrader, we treated H3122 cells with compounds **A1**, **Q2**, and **Hyt-9** to observe whether LTK and GAK would be degraded after 24 h of treatment at 0.1 or 0.5 μM. The degrader **Q2** could almost completely degrade GAK at 0.5 μM, while the degrader **Hyt-9** showed no visible effect on LTK and GAK expression levels in H3122 cells at the same concentration (Figure 7C), suggesting that the degrader **Hyt-9** appears to have a stronger selectivity than **Q2**. To further examine the proteome-wide degradative selectivity of **Hyt-9**, we performed proteomic isobaric tags for relative and absolute quantitation (iTRAQ). As shown in Figure 7D, **Hyt-9** exhibited a high selectivity for ALK among 6766 proteins except for ATP1A1, PSS2, WASF3, and thymidylate synthase (Supporting Information, Table S4), whose downregulation was further verified by western blotting (Supporting Information, Figure S10).

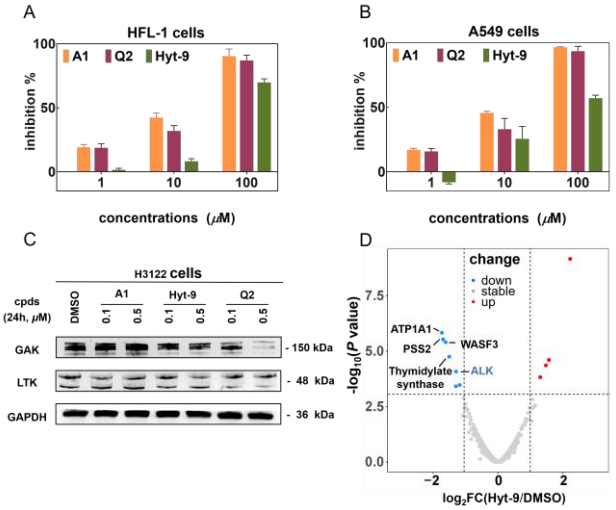

Figure 7. Selective inhibition and degradation of ALK by the degrader **Hyt-9**. Antiproliferative activity of **A1**, **Q2**, and **Hyt-9** in (A) HFL-1 and (B) A549 cells. (C) H3122 cells were treated with 0.1 or 0.5 μM **A1**, **Q2**, and **Hyt-9** for 24 h to compare the selective degradative potency of compounds against GAK and LTK. (D) Volcano plot showing changes in protein abundance. H3122 cells were treated with DMSO or 1 μM **Hyt-9** for 24 h. The proteins were analyzed by proteomic iTRAQ. The x-axis displays the relative abundance of all identified proteins (6,766) in compound **Hyt-9**-treated cells (log_2FC) vs. DMSO-treated cells. The y-axis displays p values ($-log_{10}$) from triplicate experiments.

Moreover, we further explored the applicability of norbornene, and two ALK degraders, **Hyt-11** and **Hyt-12**, were designed and synthesized based on two ALK inhibitors, ceritinib and brigatinib, by connecting norbornene through short amide linkers (Figure 8A, B, Supporting Information, Schemes S5 and S6). Immunoblotting results indicated that both **Hyt-11** and **Hyt-12** potently degraded EML4-ALK in a dose-dependent manner with DC_{50} values of 314 nM and 89 nM, respectively, after 24 h of treatment (Figure 8C, D). Furthermore, to assess whether the generality of this degradation phenomenon mediated by norbornene-based HyT could be applied to other targets, we selected EZH2 for HyT-degrader design because it is a highly compelling but intractable target for the development of antitumor agents. The oncogenic role of EZH2 in cancer is mediated mainly by both polycomb repressive complex 2 (PRC2)-independent transcriptional activation and PRC2-dependent gene silencing by catalyzing H3K27me3.[28] Currently, EZH2 inhibitors show limited efficacy owing to the lack of inhibition of PRC2-independent transcriptional activation. The TPD therapeutic strategy may shed light on the complete inhibition of EZH2 oncogenic activity.[29] Thus, we synthesized the norbornene-linked EZH2 degrader **Hyt-13** (Figure 8E, Supporting Information, Scheme S7). To our delight, **Hyt-13** significantly decreased the level of EZH2 at a concentration of 10 μM after 24 h of treatment and achieved thorough degradation at 40 μM (Figure 8F). Furthermore, the degrader **Hyt-13** resulted in a > 12-fold increase in the antiproliferative activity of MDA-MB-468 cells compared with tazemetostat, the only EZH2 inhibitor approved by the US Food and Drug Administration (FDA) (Figure 8E, Supporting Information, Figure S11A). Treatment of MDA-MB-468 cells with **JBP** (1-bicyclo[2.2.1]hept-5-en-2-ylmethanamine, norbornene derivative) or tazemetostat did not decrease EZH2 protein levels or lead to significant cell growth inhibition (Supporting Information, Figure S11B). These results indicated that our designed norbornene-based HyT molecule **Hyt-13** inhibited cell growth by acting mainly as an EZH2 degrader, which has opened up a new avenue for targeting formerly undruggable targets such as non-enzymatic proteins. Thus, the novel norbornene-based HyT substantially broadened the spectrum of TPD strategies. Undoubtedly, HyT technology shows promise for future drug development.

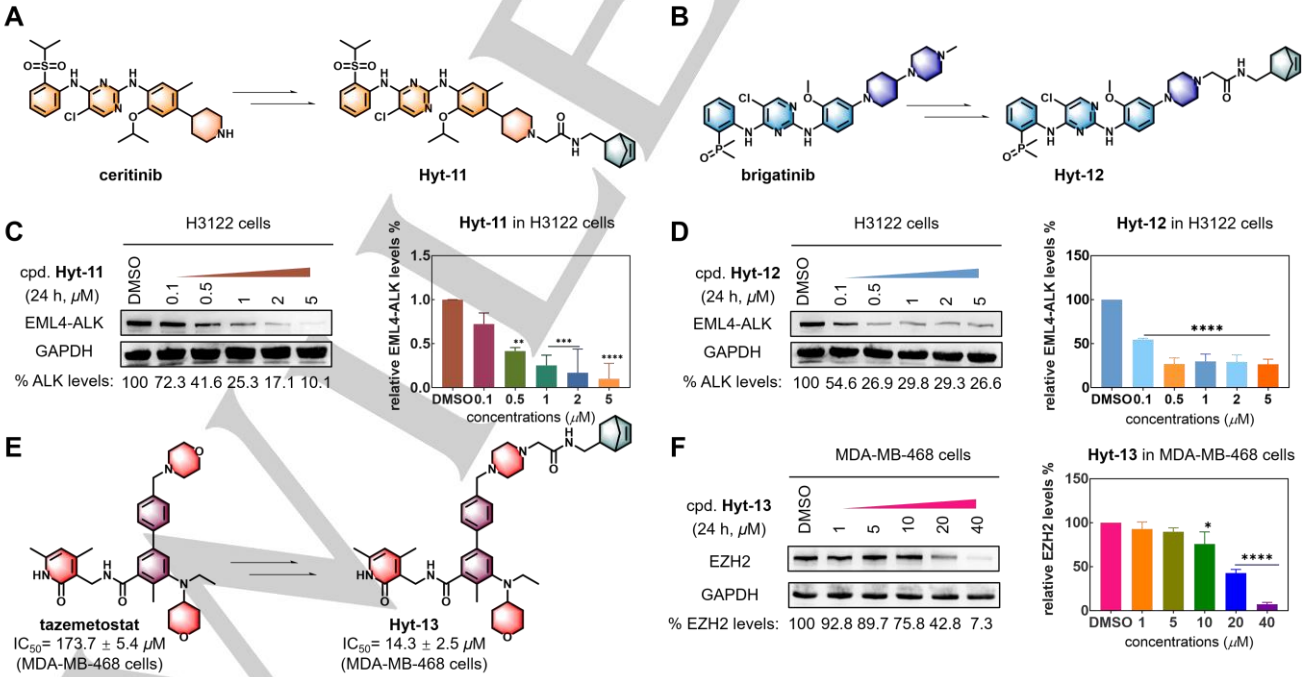

Figure 8. Design of norbornene-based HyTs from the ALK inhibitors (A) ceritinib, (B) brigatinib, and the EZH2 inhibitor tazemetostat (E). Immunoblot analyses of H3122 cells incubated with (C) **Hyt-11** and (D) **Hyt-12** for 24 h and MDA-MB-468 cells incubated with (F) **Hyt-13** for 24 h. EML4-ALK or EZH2 levels were normalized relative to those of EML4-ALK or EZH2 levels in DMSO, respectively. * p< 0.05, ** p< 0.01, *** p< 0.001, and **** p< 0.0001 vs. vehicle control.

Conclusions

TPD technology has received much attention for therapeutic intervention, especially in the field of eliminating “undruggable” protein targets such as transcription factors and non-enzymatic proteins. PROTACs represent mainstream TPD technologies and have made great progress in the degradation of disease-causing proteins. However, the potency of PROTACs has several limitations. Other classes of TPD strategies are constantly emerging and have greatly expanded the scope of TPD, including but not limited to lysosome-targeting chimeras (LYTAC),[30] antibody-based PROTAC (AbTAC),[31] autophagy-targeting chimeras (AUTACs),[32] and autophagosome-tethering compounds (ATTECs).[33] These technologies still face obstacles in terms of druggability owing to their large molecular size.

As a promising therapeutic strategy, HyT technology provides new insights into the design of TPDs for drug discovery. In this study, several novel HyT degraders of ALK were designed and synthesized by connecting different types of hydrophobic tags to the ALK inhibitor **A3**. The degrader **Hyt-9** was tagged with the novel hydrophobic tag norbornene, which has the lowest molecular weight ever reported, and showed potent antiproliferative activities and degradative potency in H3122 cells. Mechanistic studies revealed that the degrader **Hyt-9** could mediate the downregulation of EML4-ALK at the protein level by recruiting Hsp70 to mediate ubiquitylated POI, thus shuttling the proteasome for degradation. In addition, the new ALK degrader **Hyt-9** exhibited sustained cellular degradative activity upon washout in H3122 cells *in vitro* and acceptable oral bioavailability *in vivo*. Furthermore, **Hyt-9** showed potent and efficacious inhibition of tumor growth *in vivo* via I.V. or P.O. administration without any body weight loss or significant toxicity. Interestingly, the novel hydrophobic tag norbornene could also be used to degrade ALK when linked with other ALK inhibitors, such as ceritinib or brigatinib as well as to degrade EZH2 when tagged with the EZH2 inhibitor tazemetostat. Thus, norbornene may be a novel and potent hydrophobic tag with potential druggability for further modification and development in the TPD field. Although the degradative mechanism of norbornene-based HyT is still not fully understood, norbornene-based HyT provides fresh insights into drug discovery. We believe that once the assumptions of HyT technology become a reality, the process of degrading target proteins by attaching hydrophobic tags to ligands of target proteins will become an assembly line.

Conflict of Interest

The authors declare no conflict of interest.

Data Availability Statement

The data that support the findings of this study are available in the Supporting Information of this article.

Acknowledgments

This study received financial support from the National Natural Science Foundation of China (nos. 82173672, 82173679, 81874289, and 81903446), the Natural Science Foundation of Jiangsu Province (BK20190564), “Double First Class” University project of China Pharmaceutical University (CPUQNJC22), and the Postgraduate Research & Practice Innovation Program of Jiangsu Province (KYCX22_0814). We appreciate technical support by the Public Experimental Pharmacology Platform of China Pharmaceutical University, and the Cellular and Molecular Biology Center of China Pharmaceutical University.

Keywords: Protein Degradation • Hydrophobic Tags • Norbornene • Anticancer • PROTACs

[1] K. M. Sakamoto, K. B. Kim, A. Kumagai, F. Mercurio, C. M. Crews, R. J. Deshaies, *Proc. Natl. Acad. Sci. U.S.A.* **2001**, *98*, 8554-8559.

[2] L. B. Snyder, T. K. Neklesa, X. Chen, H. Dong, C. Ferraro, D. A. Gordon, *American Association for Cancer Research (AACR)* **2021**, April 10−15.

[3] a) T. K. Neklesa, J. D. Winkler, C. M. Crews, *Pharmacol. Ther.* **2017**, *174,* 138-144; b) C. Cantrill, P. Chaturvedi, C. Rynn, J. Petrig Schaffland, I. Walter, M. B. Wittwer, *Drug Discov. Today* **2020**, *25*, 969-982; c) S. D. Edmondson, B. Yang, C. Fallan, *Bioorg. Med. Chem. Lett.* **2019**, *29*, 1555-1564.

[4] A. C. Lai, C. M. Crews, *Nat. Rev. Drug Discov.* **2017**, *16*, 101-114.

[5] a) G. E. Winter, D. L. Buckley, J. Paulk, J. M. Roberts, A. Souza, S. Dhe-Paganon, J. E. Bradner, *Science* **2015**, *348*, 1376-1381; b) J. Lu, Y. Qian, M. Altieri, H. Dong, J. Wang, K. Raina, J. Hines, J. D. Winkler, A. P. Crew, K. Coleman, C. M. Crews, *Chem. Biol.* **2015**, *22*, 755-763; c) J. Wei, F. Meng, K. S. Park, H. Yim, J. Velez, P. Kumar, L. Wang, L. Xie, H. Chen, Y. Shen, E. Teichman, D. Li, G. G. Wang, X. Chen, H. Kaniskan, J. Jin, *J. Am. Chem. Soc.* **2021**, *143*, 15073-15083.

[6] a) Y. Wang, X. Jiang, F. Feng, W. Liu, H. Sun, *Acta Pharm. Sin. B.* **2020**, *10,* 207-238; b) L. M. Luh, U. Scheib, K. Juenemann, L. Wortmann, M. Brands, P. M. Cromm, *Angew. Chem., Int. Ed.* **2020**, *59*, 15448-15466.

[7] a) J. L. Gustafson, T. K. Neklesa, C. S. Cox, A. G. Roth, D. L. Buckley, H. S. Tae, T. B. Sundberg, D. B. Stagg, J. Hines, D. P. McDonnell, J. D. Norris, C. M. Crews, *Angew. Chem., Int. Ed.* **2015**, *54*, 9659-9662; b) S. M. Lim, T. Xie, K. D. Westover, S. B. Ficarro, H. S. Tae, D. Gurbani, T. Sim, J. A. Marto, P. A. Jänne, C. M. Crews, N. S. Gray, *Bioorg. Med. Chem. Lett.* **2015**, *25*, 3382-3389; c) T. Xie, S. M. Lim, K. D. Westover, M. E. Dodge, D. Ercan, S. B. Ficarro, D. Udayakumar, D. Gurbani, H. S. Tae, S. M. Riddle, T. Sim, J. A. Marto, P. A. Jänne, C. M. Crews, N. S. Gray, *Nat. Chem. Biol.* **2014**, *10*, 1006-1012; d) A. Ma, E. Stratikopoulos, K. S. Park, J. Wei, T. C. Martin, X. Yang, M. Schwarz, V. Leshchenko, A. Rialdi, B. Dale, A. Lagana, E. Guccione, S. Parekh, R. Parsons, J. Jin, *Nat. Chem. Biol.* **2020**, *16*, 214-222; e) T. K. Neklesa, H. S. Tae, A. R. Schneekloth, M. J. Stulberg, T. W. Corson, T. B. Sundberg, K. Raina, S. A. Holley, C. M. Crews, *Nat. Chem. Biol.* **2011**, *7*, 538-543.

[8] A. Go, J. W. Jang, W. Lee, J. D. Ha, H. J. Kim, H. J. Nam, *Eur. J. Med. Chem.* **2020**, *204*, 112635.

[9] M. Hachisu, A. Seko, S. Daikoku, Y. Takeda, M. Sakono, Y. Ito, *ChemBioChem.* **2016**, *17*, 300-303.

[10] a) M. J. Long, D. R. Gollapalli, L. Hedstrom, *Chem. Biol.* **2012**, *19*, 629-637; b) Y. Shi, M. J. Long, M. M. Rosenberg, S. Li, A. Kobjack, P. Lessans, R. T. Coffey, L. Hedstrom, *ACS Chem. Biol.* **2016**, *11*, 3328-3337.

[11] Y. Asawa, K. Nishida, K. Kawai, K. Domae, H. S. Ban, A. Kitazaki, H. Asami, J. Y. Kohno, S. Okada, H. Tokuma, D. Sakano, S. Kume, M. Tanaka, H. Nakamura, *Bioconjugate Chem*. **2021**, *32*, 2377-2385.

[12] J. Li, T. Liu, Y. Song, M. Wang, L. Liu, H. Zhu, Q. Li, J. Lin, H. Jiang, K. Chen, K. Zhao, M. Wang, H. Zhou, H. Lin, C. Luo, *J. Med. Chem*. **2022**, *65*, 11034-11057.

[13] H. S. Tae, T. B. Sundberg, T. K. Neklesa, D. J. Noblin, J. L. Gustafson, A. G. Roth, K. Raina, C. M. Crews, *ChemBioChem* **2012**, *13*, 538-541.

[14] N. Gao, T. T. Chu, Q. Q. Li, Y. J. Lim, T. Qiu, M. R. Ma, Z. W. Hu, X. F. Yang, Y. X. Chen, Y. F. Zhao, Y. M. Li, *RSC Adv*. **2017**, *7*, 40362-40366.

[15] M. Guo, S. He, J. Cheng, Y. Li, G. Dong, C. Sheng, *ACS Med. Chem. Lett*. **2022**, *13*, 298-303.

[16] S. R. Choi, H. M. Wang, M. H. Shin, H. S. Lim, Int. *J. Mol. Sci.* **2021**, 22, 6407.

[17] F. Xu, X. Zhang, Z. Chen, S. He, J. Guo, L. Yu, Y. Wang, C. Hou, H. Ai-Furas, Z. Zheng, J. B. Smaill, A. V. Patterson, Z. M. Zhang, L. Chen, X. Ren, K. Ding, *J. Med. Chem*. **2022**, *65*, 14032–14048.

[18] S. Rubner, A. Scharow, S. Schubert, T. Berg, *Angew. Chem., Int. Ed*. **2018**, *130*, 17289-17293.

[19] D. L. Buckley, C. M. Crews, *Angew. Chem., Int. Ed.* **2014**, *53*, 2312-2330.

[20] S. Xie, Y. Sun, Y. Liu, X. Li, X. Li, W. Zhong, F. Zhan, J. Zhu, H. Yao, D. H. Yang, Z. S. Chen, J. Xu, S. Xu, *J. Med. Chem.* **2021**, *64*, 9120-9140.

[21] a) X. Kong, P. Pan, H. Sun, H. Xia, X. Wang, Y. Li, T. Hou, *J. Med. Chem.* **2019**, *62*, 10927-10954; b) J. Chen, Y. Zhou, X. Dong, L. Liu, L. Bai, D. McEachern, S. Przybranowski, C. Y. Yang, J. Stuckey, X. Li, B. Wen, T. Zhao, S. Sun, D. Sun, L. Jiao, Y. Jing, M. Guo, D. Yang, S. Wang, *J. Med. Chem.* **2020**, *63*, 13994-14016.

[22] S. Kim, T. M. Kim, D. W. Kim, H. Go, B. Keam, S. H. Lee, J. L. Ku, D. H. Chung, D. S. Heo, *J. Thorac. Oncol*. **2013**, *8*, 415-422.

[23] R. Rosenzweig, N. B. Nillegoda, M. P. Mayer, B. Bukau, *Nat. Rev. Mol. Cell Biol.* **2019**, *20*, 665-680.

[24] a) D. R. Williams, S. K. Ko, S. Park, M. R. Lee, I. Shin, *Angew. Chem., Int. Ed.* **2008**, *47*, 7466-7469; b) S. K. Ko, J. Kim, D. C. Na, S. Park, S. H. Park, J. Y. Hyun, K. H. Baek, N. D. Kim, N. K. Kim, Y. N. Park, K. Song, I. Shin, *Chem. Biol*. **2015**, *22*, 391-403.

[25] D. M. Molina, R. Jafari, M. Ignatushchenko, T. Seki, E. A. Larsson, C. Dan, L. Sreekumar, Y. Cao, P. Nordlund, *Science* **2013**, *341*, 84-87;

[26] R. J. Roskoski, *Pharmacol. Res.* **2013**, *68*, 68-94.

[27] H. Sakamoto, T. Tsukaguchi, S. Hiroshima, T. Kodama, T. Kobayashi, T. A. Fukami, N. Oikawa, T. Tsukuda, N. Ishii, Y. Aoki, *Cancer Cell* **2011**, *19*, 679-690.

[28] R. Duan, W. Du, W. Guo, *J. Hematol. Oncol.* **2020**, *13*, 104.

[29] a) Z. Liu, X. Hu, Q. Wang, X. Wu, Q. Zhang, W. Wei, X. Su, H. He, S. Zhou, R. Hu, T. Ye, Y. Zhu, N. Wang, L. Yu, *J. Med. Chem.* **2021**, *64*, 2829-2848; b) J. Wang, X. Yu, W. Gong, X. Liu, K. S. Park, A. Ma, Y. H. Tsai, Y. Shen, T. Onikubo, W. C. Pi, D. F. Allison, J. Liu, W. Y. Chen, L. Cai, R. G. Roeder, J. Jin, G. G. Wang, *Nat. Cell Biol.* **2022**, *24*, 384-399.

[30] G. Ahn, S. M. Banik, C. L. Miller, N. M. Riley, J. R. Cochran, C. R. Bertozzi, *Nat. Chem. Biol.* **2021**, *17*, 937-946.

[31] A. D. Cotton, D. P. Nguyen, J. A. Gramespacher, I. B. Seiple, J. A. Wells, *J. Am. Chem. Soc.* **2021**, *143*, 593-598.

[32] D. Takahashi, J. Moriyama, T. Nakamura, E. Miki, E. Takahashi, A. Sato, T. Akaike, K. Itto-Nakama, H. Arimoto, *Mol. Cell* **2019**, *76*, 797-810.

[33] Y. Fu, N. Chen, Z. Wang, S. Luo, Y. Ding, B. Lu, *Cell Res.* **2021**, *31*, 965-979.

Entry for the Table of Contents

Norbornene was first developed as a novel hydrophobic tag to expand the clinical potential of TPD technologies. The novel degrader **Hyt-9** was obtained by connecting an ALK ligand with norbornene, which exhibited potent antiproliferative and degradative activities *in vitro* and *in vivo*. Furthermore, norbornene could be used to degrade EZH2 when tagged with the EZH2 inhibitor tazemetostat **Hyt-13**.

WILEY-VCH